IEEE Access
Multidisciplinary | Rapid Review | Open Access Journal

Received September 4, 2019, accepted October 4, 2019, date of publication October 11, 2019, date of current version October 25, 2019.

Digital Object Identifier 10.1109/ACCESS.2019.2946747

Improved Restricted Control Set Model Predictive Control (iRCS-MPC) Based Maximum Power Point Tracking of Photovoltaic Module

AFAQ HUSSAIN[1], HADEED AHMED SHER[1], (Senior Member, IEEE), ALI FAISAL MURTAZA[2], (Member, IEEE), AND KAMAL AL-HADDAD[3], (Fellow, IEEE)

[1]Faculty of Electrical Engineering, Ghulam Ishaq Khan Institute of Engineering Sciences and Technology, Topi 23460, Pakistan
[2]Faculty of Engineering, University of Central Punjab, Lahore 54000, Pakistan
[3]Ecole de Technologie Superieure, Montreal, QC H3C 1K3, Canada

Corresponding author: Hadeed Ahmed Sher (hadeedsher@ieee.org)

This work was supported by the Higher Education Commission (HEC) of Pakistan through the Start-up Research Grant Program (SRGP), under Project 21-1764/SRGP/R&D/HEC/2017.

ABSTRACT This paper presents a robust two stage maximum power point tracking (MPPT) system of the photovoltaic (PV) module using an improved restricted control set model predictive control (iRCS-MPC) technique. The suggested work is improved in two aspects; a revision in conventional P&O algorithm is made by employing three distinct step sizes for different conditions, and an improvement in conventional MPC algorithm. The improved MPC algorithm is based on the single step prediction horizon that provides less computational load and swift tracking of maximum power point (MPP) by applying the control pulses directly to the converter switch. The computer aided experimental results for various environmental scenarios revealed that compared with the conventional method (conventional P&O + MPC), for the PV power and inductor current, the undershoot and overshoot is decreased to 68% and 35% respectively under stiff environmental conditions. In addition, the settling time needed to reach a stable state is significantly reduced in the proposed system. The viability of the solution suggested is verified in MATLAB/Simulink and by hardware experimentation.

INDEX TERMS Boost converter, dc-dc power conversion, maximum power point tracking (MPPT), MPC, photovoltaic systems, model predictive control (RCS-MPC).

I. INTRODUCTION

The power harnessed by the PV unit is non-linear and dependent on the environmental conditions. Therefore, impedance matching is performed electronically to fetch maximum power from the PV module. Usually, load is matched with the PV module using a dedicated power electronic interface, for example a boost converter. A boost converter, matches the source impedance with the load impedance using software defined algorithms known as maximum power point tracking (MPPT) methods. Such algorithms record the reference variable in either current, voltage or the duty cycle and transfer to the controller the relevant output.

The most commonly used methods for MPPT are the hill climbing methods i.e., perturb and observe (P&O) and incremental conductance (InC) method [1]–[4]. Among these two, P&O is considered simple, flexible and more advantageous for commercial applications [5]. Conventional P&O methods, however, generate power oscillations under regular and volatile weather conditions. To solve these issues, researchers in [6], [7] recommended various strategies to follow the photovoltaic voltage using feedback system. Since the irradiation and photovoltaic current(I_{pv}) are linked together, in [8]–[10] the current is chosen as a control variable. However, under fast changing irradiation, the control system may lead the operating variable in the wrong direction, a phenomenon called drifting. The drifting phenomenon is mitigated in a revised sliding mode control (SMC) based P&O with voltage rectification loop [8]. In [11] an MPPT algorithm is presented that links the fractional short circuit current (FSCC) MPPT method to the conventional P&O. A model predictive controller (MPC) based MPPT is recommended in [10] wherein an MPC predicts the subsequent error. An appropriate control variable is applied to a dc-dc

The associate editor coordinating the review of this manuscript and approving it for publication was Liu Hongchen.

TABLE 1. Comparison of different controllers used to track MPP.

MPPT technique	Modulation	Advantage	Disadvantage	Reference
P&O technique	Pulse width modulation (PWM)	easy implementation	Power oscillation under dynamic weather condition	[1], [15]
Incremental conductance technique	PWM	Control efficiency is better than P&O	Not reliable	[16], [17]
Fractional short circuit current	PWM	Perturbation is not required	Efficiency reduces	[11], [18]
Fractional open circuit voltage	PWM	Perturbation is not required	Accuracy is reduced with respect to module parameters degradation	[19], [20]
Fuzzy logic based MPPT	PWM	Better tracks the MPP because of nonlinear control accuracy	Large computational load on controller and difficult to implement practically	[21], [22]
Sliding mode control based MPPT	PWM	High control efficiency than the previous techniques	Difficult to implement practically	[8], [23]
MPC based MPPT	MPC pulses	Fast Transient response	Small undershoot and overshoot under rapid change in irradiance	[24]
Proposed modified MPC based MPPT	MPC pulses	No undershoot and overshoot under rapid change in irradiance	Not tested for grid connected application	Proposed paper

boost converter to mitigate the future error. In [12], [13] fuzzy logic controller (FLC) for PV applications is presented. However, implementing FLC is practically a complex process because of high computational load requirement [14].The comparison of different MPPT techniques in literature is given in Table 1.

In the proposed work, an improved P&O algorithm based MPPT is combined with an improved restricted control set MPC (iRCS-MPC) controller. The proposed control technique reduces the implementation complexity for controller design and does not include inner control loops and inflectors [25]. Moreover, use of restricted control set enjoys the modulator less operation and send the pulses directly to the boost converter. This uses a predictive limit to forecast the system's future behavior by correctly modeling the practical system [26]. From the future behavior, the control algorithm decides the instantaneous input for which the instantaneous output is close to the desired output. In the proposed iRCS-MPC, only one step prediction limit is adopted to track the MPP. The paper presented makes an important contribution in minimizing the transients (% undershoot and overshoot) of the module current. Therefore, the power oscillations are significantly reduced without increasing the MPC workload. The remaining paper is organized according to the following scheme: Section II explains the PV system. Section III presents detailed modeling of the proposed system. Section IV explains the proposed approach. The concept validation of proposed and conventional method is exhibited under different simulation scenarios section V. In section VI, the validation of the proposed work is verified through hardware prototype.

II. PV SYSTEM DESCRIPTION

The proposed system is shown in Fig. 1. It includes a PV module, a dc-dc boost converter, resistive load and a control block. The inductor current (I_L), photovoltaic voltage (V_{pv}) and load voltage (V_o) are sensed using voltage and current sensors are used as input for the iRCS-MPC block. Note that the MPP tracker generates the reference current as output variable. The output of the iRCS-MPC block is used to gate the mosfet. α and β in $G_{s=0}$ and $G_{s=1}$ are weighting factors that depends upon the priorities that are given to the different future errors in cost function (CF). V^* is the reference output voltage that is the numerical value provided by the user.

III. PV SYSTEM MODELING

A. BOOST CONVERTER MODELING

Mathematical modeling in terms of state-space is desired for realizing the proposed iRSC-MPC system. The modeling is performed on the guidelines provided in [27]. Based on the gating signal of the switch Q, a boost converter can have two equivalent circuits as shown in Fig. 2. Note that in Fig. 1, the control variables of the boost converter are I_L and V_o.

During the switch off mode, the switch Q is open. The equivalent circuit shown in Fig. 2a can be mathematically expressed in terms of control variable as

$$\frac{dI_L}{dt} = -\frac{1}{L}.V_o + \frac{1}{L}.V_{pv} \tag{1}$$

$$\frac{dV_o}{dt} = \frac{1}{C}.I_L - \frac{1}{R_L.C}.V_o \tag{2}$$

R_L represents the load resistance. To avoid mismatching condition and to improve the performance of the system, R_L should be calculated at each sampling instant. The calculation of R_L is given as follows:

$$D = 1 - (\frac{V_{pv}}{V_c}) \tag{3}$$

$$i_o = i_L.(1 - D) \tag{4}$$

where i_o represents the output current

$$R_L = \frac{V_c}{i_o} \tag{5}$$

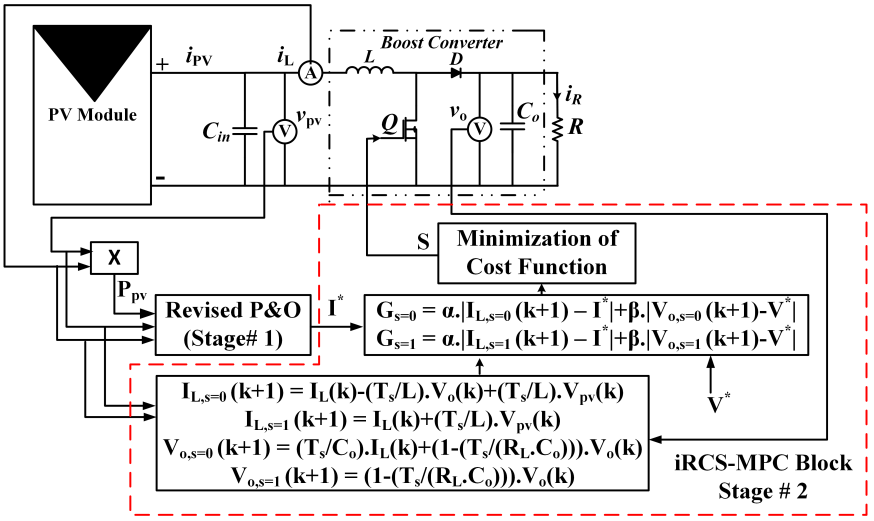

FIGURE 1. Concept diagram of the proposed work.

During the switch on mode, the switch Q is closed and therefore it can be modeled as a short circuit path. During this mode the control variables I_L and V_o are given as

$$\frac{dI_L}{dt} = \frac{1}{L}.V_{pv} \tag{6}$$

$$\frac{dV_o}{dt} = -\frac{1}{R_L.C}.V_o \tag{7}$$

Equations eq. (1)-(7) are transformed into a discrete domain for the practical use through the Euler equation as shown in eq.(8).

$$\frac{dz(t)}{dt} \approx \frac{z(k+1) - z(k)}{T_s} \tag{8}$$

where, k is the sampling instant and T_s is the sampling period. Using eq.(8), eq. (1)- (7) can be discretized as follows:

$$I_{L,s=0(k+1)} = I_L(k) - \frac{T_s}{L}.V_o(k) + \frac{T_s}{L}.V_{pv}(k) \tag{9}$$

$$V_{o,s=0(k+1)} = \frac{T_s}{C}.I_L(k) + (1 - \frac{T_s}{R_L.C}).V_o(k) \tag{10}$$

$$I_{L,s=1(k+1)} = I_L(k) + \frac{T_s}{L}.V_{pv}(k) \tag{11}$$

$$V_{o,s=1(k+1)} = (1 - \frac{T_s}{R_L.C}).V_o(k) \tag{12}$$

Note that the variable C represents the output capacitor C_o, L represents the inductor as shown in Fig.2. The eq.(9-12) can be rearranged as eq.(13).

$$\begin{bmatrix} I_{L(k+1)} \\ V_{o(k+1)} \end{bmatrix} = \begin{bmatrix} 1 & -(1-s).\frac{T_s}{L} \\ (1-s).\frac{T_s}{C} & (1 - \frac{T_s}{R_L.C}) \end{bmatrix} \cdot \begin{bmatrix} I_{L(k)} \\ V_o(k) \end{bmatrix} + \begin{bmatrix} \frac{T_s}{L} \\ 0 \end{bmatrix} V_{pv(k)} \tag{13}$$

where the switching condition of "s" is equivalent to 1 when switching on mode and 0 when switching off. Note that the performance of state variables I_L and V_o is projected to calculate the control sequence for the present and future sampling points.

IV. PROPOSED SCHEME (REVISED P&O + IRCS-MPC)

This section explains the proposed method (Revised P&O + iRCS-MPC) in contrast with the conventional method (conventional P&O + MPC). The proposed MPPT algorithm is a two stage scheme wherein, the first stage is the revised P&O and the second stage is the restricted control set MPC. The working of the stage I and II is explained below.

A. STAGE I | THE REVISED P&O APPROACH

The proposed MPPT method modifies the conventional P&O method in two aspects. First, it has two distinct step size values for various conditions. The I_{inc1} is for normal P&O operation and I_{inc2} is the step size for abrupt as well as for gradual change (Ramp shape) in irradiance. Secondly, the distinction between the gradual and sudden irradiance condition is made through a power limit that compares the power difference (ΔP) with the predefined power band (P_{set}). The working of this stage is as follows.

The system starts by measuring the photovoltaic voltage (V_{pv}) and inductor current (I_L) and calculates the instantaneous power (P_{pv}). The algorithm then calculates the change in photovoltaic voltage (ΔV), current (ΔI), and power (ΔP). The flowchart of the proposed system is shown in Fig.3.There are three different environmental conditions which is to be tackled by the proposed algorithm in stage I, the working of the proposed algorithm in stage I for three different environmental conditions are given as follows:

1) NORMAL IRRADIANCE

In this condition, the condition ($\Delta I >= I_{set}$) is violated because I_{set} indicates the occurrence of gradual or abrupt change in irradiance, then ($I_{inc} = I_{inc1}$) is selected and then the second conditional block ($\Delta P > P_{set}$) is also violated because P_{set} indicates the occurrence of abrupt change in irradiance. After that the conventional P&O is

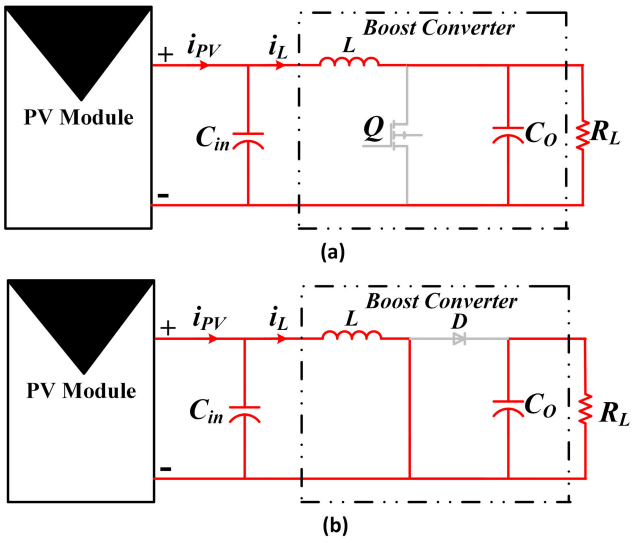

FIGURE 2. Boost converter equivalent circuit for switch mode a) OFF and b) ON.

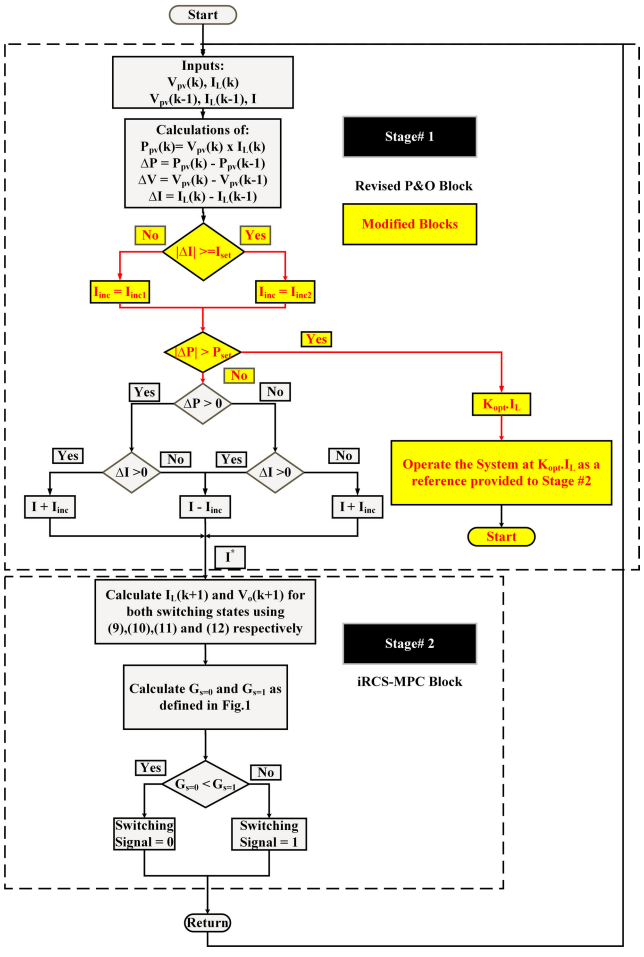

FIGURE 3. Flowchart of the revised P&O approach.

executed which provides I^* for stage II. The working mechanism of proposed approach in normal irradiance condition is explained in Fig. 4.

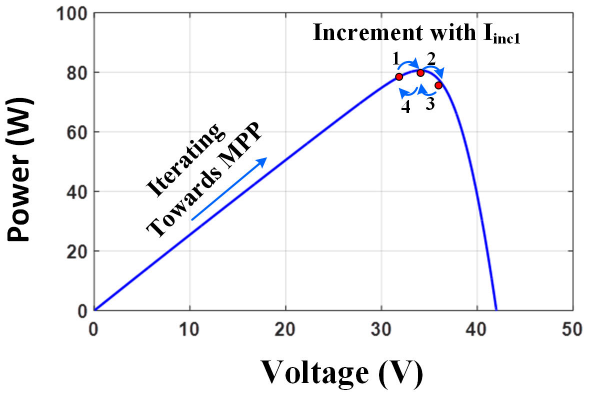

FIGURE 4. Operating process of proposed method in normal irradiance condition.

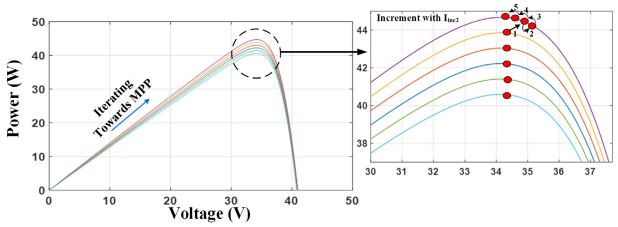

FIGURE 5. Operating process of proposed method in gradual irradiance change condition.

2) GRADUAL IRRADIANCE CHANGE (RAMP SHAPE)

In this condition, the condition ($\Delta I >= I_{set}$) ia fulfilled because I_{set} indicates the occurrence of gradual or abrupt change in irradiance, then ($I_{inc} = I_{inc2}$) is selected and then the second conditional block ($\Delta P > P_{set}$) is violated because P_{set} indicates the occurrence of abrupt change in irradiance. After that the conventional P&O is executed which provides I^* for stage II.The working mechanism of proposed approach in gradual irradiance change condition is explained in Fig. 5.

3) ABRUPT IRRADIANCE CHANGE

In this condition, the conditional block ($\Delta I >= I_{set}$) is set true and ($I_{inc} = I_{inc2}$) is selected. In this case the second conditional block ($\Delta P > P_{set}$) is also fulfilled because P_{set} indicates the occurrence of abrupt change in irradiance. In the first iteration, the stage I block provides the inductor current multiplied with K_{opt} which is the optimum scaling factor as a reference current for stage II. This is done by turning on the MOSFET for somewhat extended period of time and it is synonymous to the concept of fractional short circuit current MPPT as expressed in eq.(14). The system is operated at this approximate MPPT and the reference is provided to stage 2. This is the instant when the ($I_L = I_{pv} = I_{scc}$), as evident from Fig.2b.The working mechanism of proposed approach in abrupt irradiance change condition is explained in Fig. 6.

$$I_L \approx K_{opt}.I_{scc} \tag{14}$$

where, I_{scc} is the measured short circuit current, K_{opt} is the optimum scaling factor with normal values between 0.80 to 0.92 [9], [28].

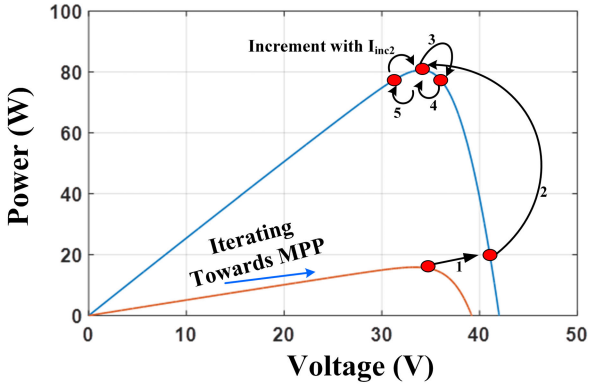

FIGURE 6. Operating process of proposed method in abrupt irradiance change condition.

Stage 2 then receives the reference current as defined in eq. (14) until $\Delta P <= P_{set}$ condition become fulfilled and then the algorithm jumps to the normal irradiation condition. After execution of stage I, the algorithm moves on to the stage II. The algorithm then moves on to the stage II (MPC block).

B. STAGE II | IMPROVED RESTRICTIVE CONTROL SET MODEL PREDICTIVE CONTROL

The reference current calculated in stage I is used in addition to the instantaneous photovoltaic current, voltage and output voltage. The future values of I_{pv} and V_o are predicted using eq.(10-13). The future values are then used to calculate $G_{s=0}$ and $G_{s=1}$ using the following procedure.

A general expression of CF for MPC algorithm which encompass the prediction step of M time steps is formulated as:

$$G_{cf} = \sum_{i=k}^{k+M-1} (|| V_o(i) ||)^2 + u_{lim}(i) \tag{15}$$

where $|| V_o ||^2$ is the predicted future error for the control variable in the form of Eucladian 2-norm, u_{lim} is the constraint on current as defined below:

$$u_{lim}(i) = \begin{cases} 0 & \text{if } I <= I_{min} \\ \text{inf} & \text{if } I >= I_{max}. \end{cases} \tag{16}$$

In the proposed iRCS-MPC, the time step used in (15) is limited to 1, consequently, Eq.(15) turns as follows:

$$G_s = \alpha. \mid I_{Ls(k+1)} - I^* \mid + \beta. \mid V_{os(k+1)} - V^* \mid \tag{17}$$

where, 's' represents the switch status, either it is 0 or 1. Coefficients α and β represents the weighting factors of current and voltage respectively.The working mechanism of iRCS-MPC is shown in Fig. 7 for inductor current and output voltage.

C. SELECTION OF P_{SET} FOR ABRUPT CHANGE IN THE IRRADIATION

The sudden change in irradiance greater than 100 W/m^2 is to be considered as abrupt irradiation change and in this case the

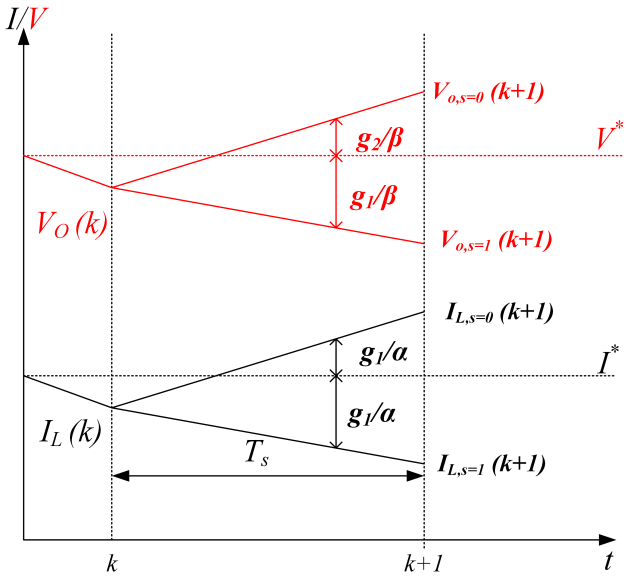

FIGURE 7. Working mechanism of iRCS-MPC technique for inductor current.

modified part of P&O algorithm in Fig.3 comes in action to quickly track the MPP. Selection of P_{set} depends upon the sampling time that is used in the MPC based PV system. In simulations, it has to be checked as to how the value of ΔP changes at 100 W/m^2 of abrupt change in irradiance, note down the value of ΔP at the point of abrupt change and select the particular value of ΔP as P_{set}. Lower the sampling time, lower will be the value of P_{set}.

D. SELECTION CRITERIA FOR I_{SET}

The slope of 3 W/m^2 is considered to be a gradual change in irradiance. Selection of I_{set} depends upon the sampling time that is used in the MPC based PV system. In simulations it has to be check that during gradual change in irradiance, how the value of ΔI changes in one iteration. Note down the value of ΔI at that point and select the particular value as I_{set}. Lower the sampling time, lower will be the value of I_{set}.

E. SELECTION CRITERIA FOR WEIGHTING FACTOR α AND β

In simulations, α and β is varied from 0 to 1 with the step of 0.1, then note down the average inductor current error and average output voltage error for each combination of α and β. Plot the graph of α vs β vs absolute average inductor current error and α vs β vs absolute average output voltage error as shown in the average inductor current increases the average output voltage as shown in Fig. 8. From Fig. 8, select the combination of α and β so that the average inductor current error and average output voltage error is within the desired range for the particular application. In this work, inductor current is given more importance because it is involved in MPPT algorithm. The selected combination of α and β are 0.89 and 0.14 respectively.

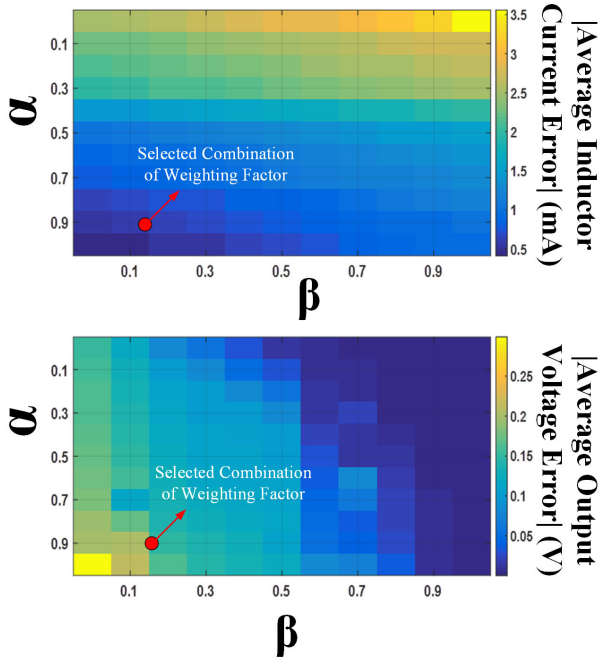

FIGURE 8. α vs β vs |average inductor current error| and α vs β vs |average output voltage error|.

TABLE 2. Parameter summary.

Specification	Variable	Value
PV module specifications		
PV module	BIPV BIPV050-S11	49.68 W
Maximum voltage	V_{oc}	8.66 V
Maximum Current	I_{sc}	8.01 A
MPP voltage	V_{mpp}	6.66 V
MPP current	I_{mpp}	7.46 A
Boost converter		
Inductor	L	4.5 mH
Input Capacitor	C_{in}	1000 μF
Output Capacitor	C_o	100 μF
Load Resistance	R_l	8 Ω
Sampling time	T_s	40μs
Increment	I_{inc1}	0.1
Increment	I_{inc2}	0.05

V. CONCEPT VALIDATION

The proposed scheme is evaluated thoroughly using numerical simulations in MATLAB/Simulink and hardware prototype built in the laboratory. The results obtained through numerical simulations were benchmarked with the conventional P&O + MPC method. A boost converter with the specifications are presented in table 2 is used to interface the PV source with the load. Notice that the weighting factor of current is more than the weighting factor of votlage. This indicates that the system is prioritized for the current control in particular. Note that from all the calculations of settling time, undershoot and overshoot for the respective testing condition, the minimum value of each is the best case scenario and maximum value is the worst case scenario.

The circuit shown in Fig.1 is tested and analyzed under six different environmental condition cases for 3s time. The obtained results for P_{pv} and I_L are plotted on the same graph

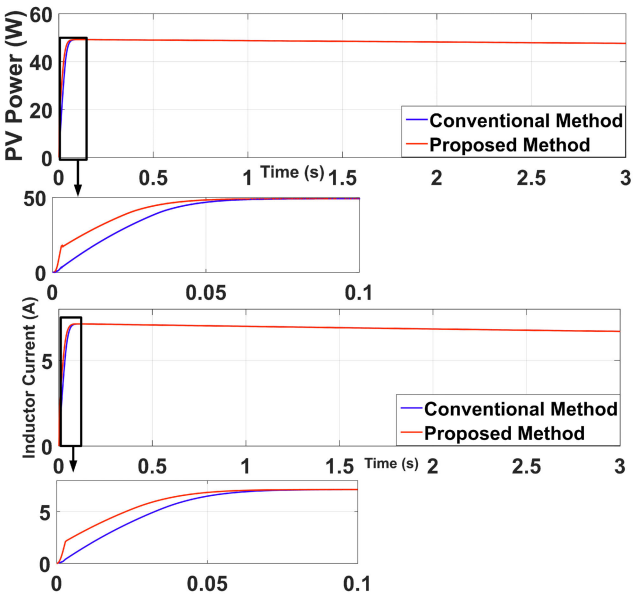

FIGURE 9. System performance under case # 1.

TABLE 3. Comparison between conventional and proposed Approach for case # 1 (Note: O/S is overshoot).

Specifications	Conventional	Proposed
% of O/S in PV power	0%	0%
Settling time	50 ms	66 ms

for performance comparison. Moreover, the formula for percentage undershoot(US) and overshoot(OS) is based on the eq.(18) and eq.(19)

$$\%US = \frac{|Amp\ osc - std\ amp| \times 100}{std\ osc} \tag{18}$$

$$\%OS = \frac{|\ value\ after\ osc - peak\ osc| \times 100}{peak\ osc} \tag{19}$$

where, amp is amplitude, osc is oscillation,std represents steady.

A. CASE # 1

This case represents the standard testing conditions for PV panels i.e., 1000 $\frac{W}{m^2}$ irradiance and 25 °C temperature. The results for both conventional and proposed approach is shown in Fig.9.

The comparison between the conventional and proposed approach for testing condition # 1 is given in Table 3.

B. CASE # 2

Case two represents abrupt increase, decrease and gradual increase, decrease in irradiance while maintaining the temperature at 25 °C. The irradiation pattern is suddenly and gradually reduced from 1k $W/m^2$to 0.7k W/m^2 and then from 0.7k W/m^2 to 1k W/m^2 as shown in Fig.10. The system outcome for proposed and conventional approach is shown in Fig. 11. The comparison between the conventional and proposed approach under case # 2 is given in Table 4.

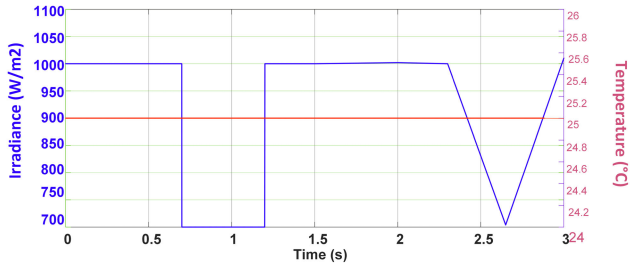

FIGURE 10. Environmental conditions for testing condition # 2.

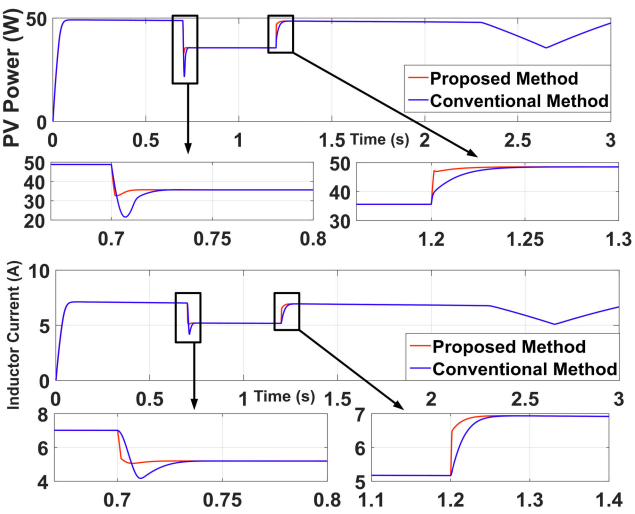

FIGURE 11. Simulated outcome of PV system under testing condition #2.

TABLE 4. Comparison of conventional method and proposed approach for case # 2 (Note: U/S is undershoot and O/S is overshoot).

Specifications	Conventional	Proposed
% of U/S in PV power under abrupt change in irradiation	43%	11%
Settling time in case of sudden decrease in PV power	26 ms	6 ms
% of O/S in PV power under abrupt change in irradiation	0%	0%
Settling time in case of sudden increase in irradiation in PV power	40 ms	1 ms
% of U/S in I_L in case of sudden irradiation change	24%	4%
Settling time of I_L if irradiation unexpectedly reduces	30 ms	5 ms
% of O/S in I_L in case of sudden irradiation change	0%	0%
Settling time of I_L if irradiation unexpectedly increases	55 ms	35 ms

C. CASE # 3

In case #3, the irradiation pattern simulates a step change in irradiance at the rate of 100 W/m^2 every 0.15s till zero. Afterwards it simulates an increment at the rate of 100 W/m^2 every 0.15s till 1000 W/m^2. Note that the temperature is fixed at 25 °C. The environmental conditions for case #3 is shown in Fig. 12. The system response for both the proposed and conventional approach under case #3 is shown in Fig. 13. The contrast between the two methods is shown in the Table 5.

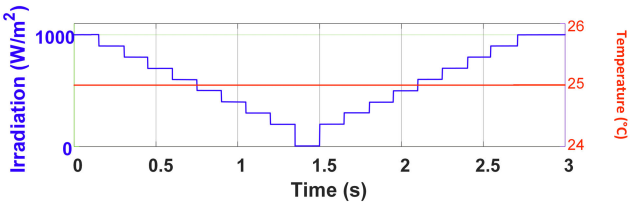

FIGURE 12. Environmental conditions for testing condition #3.

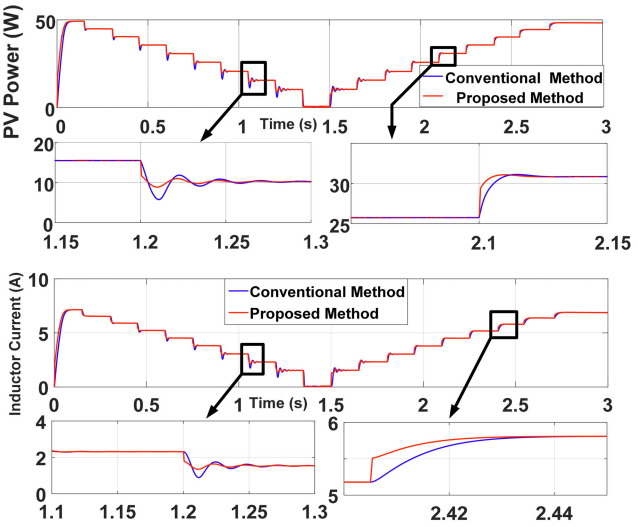

FIGURE 13. Simulated outcome of PV system under testing condition #3.

D. ROBUSTNESS OF THE PROPOSED SYSTEM

The robustness of the proposed system with respect to the conventional system is being determined from the phase portrait plot that is plotted under rapid step change in irradiance from 0 to 800 W/m^2 as shown in Fig. 14. From Fig. 14, it is analyzed that the derivative of output power is much smaller in proposed system as compared to conventional system which means that overshoot is larger in conventional system than proposed system. Moreover, the outer most circle rounds at 58W in conventional system while outermost circle rounds at 62.7W power which means that proposed system achieve stable condition having less oscillations than the conventional system.

The effect of change in output capacitance and inductor due to the effect of change in temperature or some non-linearities in the system on average inductor current is shown in Fig.15. It is analyzed from Fig.15 that average inductor current error have not much impact on distracting the MPP from its original point.

In conventional method, R_L in the algorithm is constant throughout the operation while in proposed system R_L is calculated in each sampling instant. The effect of change in R_L due to the change in temperature or other non-linearities in the system on average inductor current error and average output voltage error is shown in Fig. 16 and it is analyzed that in conventional system, change in load resistance have much effect on distracting the system from original MPP.

TABLE 5. Comparison of conventional method and proposed approach for case # 3(Note: U/S is undershoot and O/S is overshoot).

Specifications	Conventional	Proposed
% of U/S in PV power in case of sudden decrease in irradiation (Best Case)	5%	0%
% of U/S in PV power in case of sudden decrease in irradiation (Worst Case)	44%	22%
% of O/S in PV power in case of sudden increase in irradiation (Best Case)	0%	0%
% of O/S in PV power in case of sudden increase in irradiation (Worst Case)	33%	18%
Settling time in case of sudden decrease in PV power (Best Case)	9 ms	5 ms
Settling time in case of sudden decrease in PV power (Worst Case)	83 ms	49 ms
Settling time in case of sudden increase in PV power (Best Case)	7 ms	4 ms
Settling time in case of sudden increase in PV power (Worst Case)	59 ms	33 ms
% of U/S in I_L in case of sudden irradiation change (Best Case)	0%	0%
% of U/S in I_L in case of sudden irradiation change (Worst Case)	35%	19%
% of O/S in I_L in case of sudden irradiation change (Best Case)	0%	0%
% of O/S in I_L in case of sudden irradiation change (Worst Case)	22%	17%
Settling time in case of sudden decrease in irradiation in I_L (Best Case)	7 ms	5 ms
Settling time of I_L if irradiation unexpectedly reduces(Worst Case)	82 ms	51 ms
Settling time in case of sudden increase in irradiation in I_L (Best Case)	7 ms	4 ms
Settling time in case of sudden increase in irradiation in I_L (Worst Case)	81 ms	47 ms

E. ANALYSIS OF COMPUTATIONAL TIME OF THE RECOMMENDED APPROACH

Figure 18 shows the pseudo code for calculating the computational time complexity. Here, N denotes the time step of MPC algorithm. In Fig. 18, cost of each executed command in a continuous loop is presented through which, the total time complexity function W(n) of proposed scheme is calculated as follows:

$$W(n) = c0 * 1 + c1 * 1 + (c2 * 2^N + 1)(c3 * 1 + c4 * 1 + c5 * 1 + c6 * 1 + c7 * 1) + c8 * 1 + c9 * 1 \quad (20)$$

where c0-c9 is the time utilized by the controller to undergo a given instruction with best,average and worst case scenario.

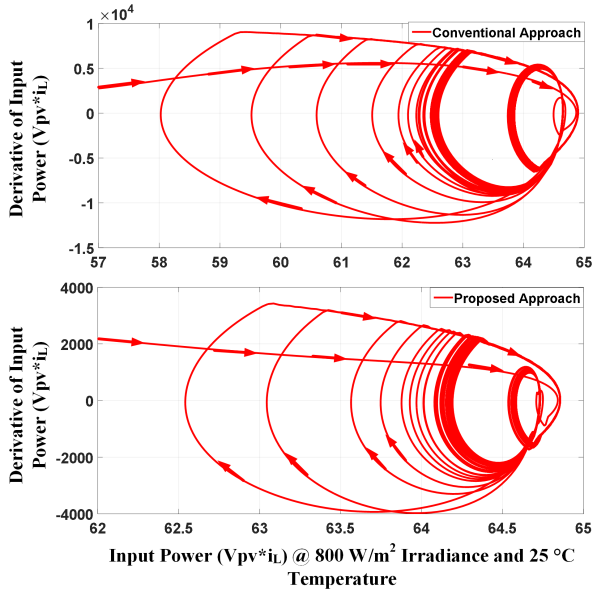

FIGURE 14. Phase portrait of proposed and conventional system under rapid step increase of irradiance from 0 t0 800 W/m^2.

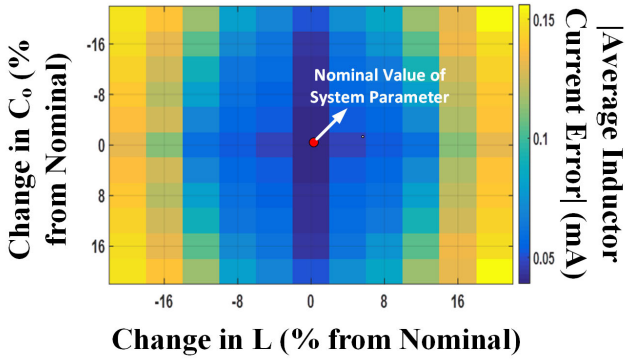

FIGURE 15. Effect of change in output capacitor and inductor on average inductor current.

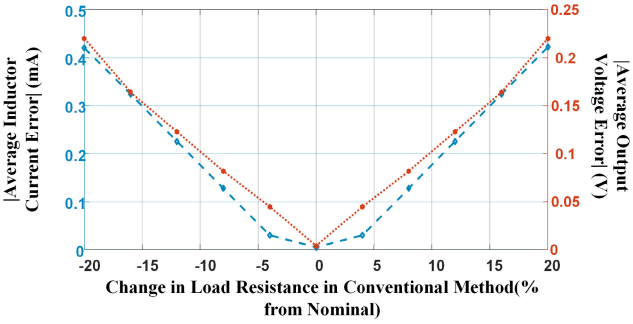

FIGURE 16. Effect of change in load resistance on average output voltage error and average inductor current error.

After solving, the (20) becomes

$$W(n) = c0 + c1 + c8 + c9 + c2 * c3 * 2^N + c2 * c4 * 2^N + c2 * c5 * 2^N + c2 * c6 * 2^N + c2 * c7 * 2^N + c3 + c4 + c5 + c6 + c7 \quad (21)$$

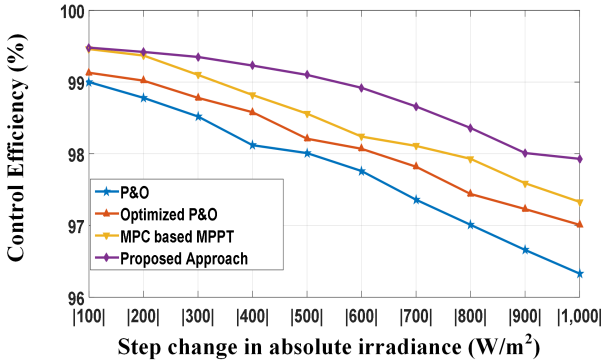

FIGURE 17. Control Efficiency among different MPPT techniques.

```
Main Program
{
  Collecting data from sensors ---> Cost = c0*1
     Execution of Stage # I    ---> Cost = c1*1
  For(int i=1;i<2^N;i++) ---> Cost = c2*(2^N+5)
   {  Eq. (7) ---> Cost = c3*1
      Eq. (8) ---> Cost = c4*1
      Eq. (9) ---> Cost = c5*1
      Eq. (10)---> Cost = c6*1
      Calculating Cost Function ---> Cost = c7*1
   }
  Select the minimum value of Cost Function ---> Cost = c8*1
  Applying the Switching State ---> Cost = c9*1
}
```

FIGURE 18. Pseudo code to calculate the computational burden.

In the presented algorithm, to minimize the computational burden, the value of N is kept to 1 therefore (21) becomes

$$W(n) = c0 + c1 + c8 + c9 + c2 * c3 * 2 + c2 * c4 * 2 + c2 * c5 * 2 + c2 * c6 * 2 + c2 * c7 * 2 + c3 + c4 + c5 + c6 + c7 \quad (22)$$

Note that larger the time step more is the value of W(n) and hence the computational load.

The comparison of the control efficiency among P&O in [15], Optimized P&O in [29], MPC based MPPT in [24] and proposed approach for different step change in irradiance is shown in Fig. 17. It is analyzed from Fig. 17 that upto absolute step change in irradiance of 200 W/m^2, control efficiency is almost equal to the control efficiency in MPC based MPPT, but it is significantly changed when step change in irradiance is increased and that is due to the modification in the flowchart of the proposed system that is shown in Fig. 3.

VI. EXPERIMENTAL VALIDATION OF PROPOSED METHOD

The experimental setup for the feasibility of the proposed method is shown in Fig. 19.The parameters used in the experimental setup is given in Table. 6. Stm32F407-Discovery is

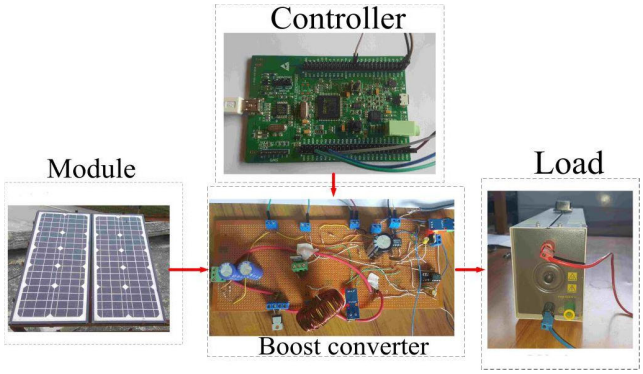

FIGURE 19. Experimental setup.

TABLE 6. Detail of prototype components.

Component	Variable	Value
2 PV module in series	BIPV BIPV040-S11	40 W each
Open circuit voltage	V_{oc}	38 V
Short Circuit Current	I_{scc}	2.57 A
Voltage at MPP	V_{mpp}	33.78 V
Current at MPP	I_{mpp}	2.37 A
Inductor	L	2.67 mH
Input Capacitor	C_{in}	1000 μF
Output Capacitor	C_o	200 μF
Load Resistance	R_L	62.5 Ω
Sampling time	T_s	100 μs

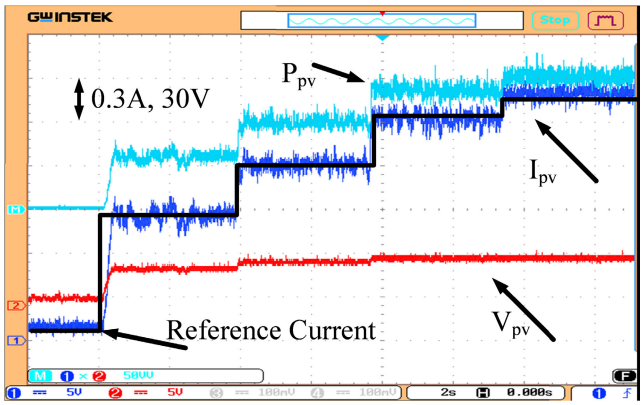

FIGURE 20. Experimental graph for different reference current (from down to up).

used for the implementation of the proposed algorithm to generate the gating signal to drive the MOSFET in boost converter. Variable rheostat (0-100) Ω is used as a DC load in the experimental setup. The proposed system was tested for different reference current on normal sunny day as shown in Fig. 20 and 22, which shows tracking capability of the proposed system for different reference current. The result of conventional P&O system is expressed in Fig.21. It is visible that the conventional P&O method suffers from overshoot during change in reference current. In Fig.23, at t0, the proposed system tracked the MPP at the practical environmental conditions at that time and at t1, the PV module is artificially shaded as shown in Fig.24 and the tracking

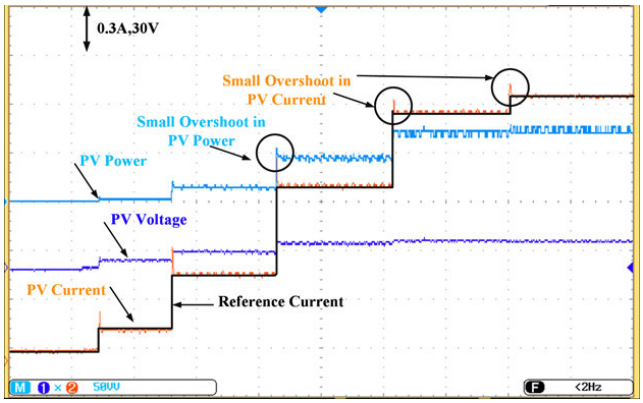

FIGURE 21. Experimental graph for conventional P&O against reference current (from down to up).

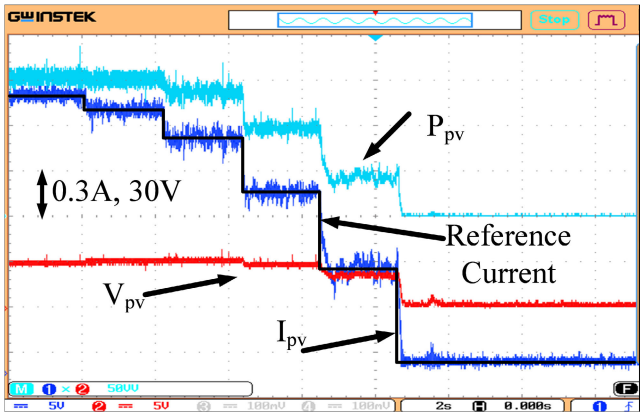

FIGURE 22. Experimental graph for different reference current (from up to down).

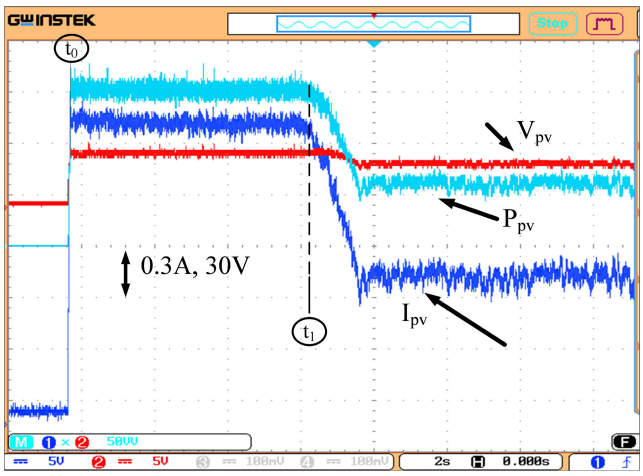

FIGURE 23. Experimental graph for MPP tracking and artificial shading applied.

capability after PV module shading is also shown in it. If we analyze Fig.20, 22 and 23, it is proved that there is negligible overshoot and undershoot in PV power after step and gradual change in the reference current.

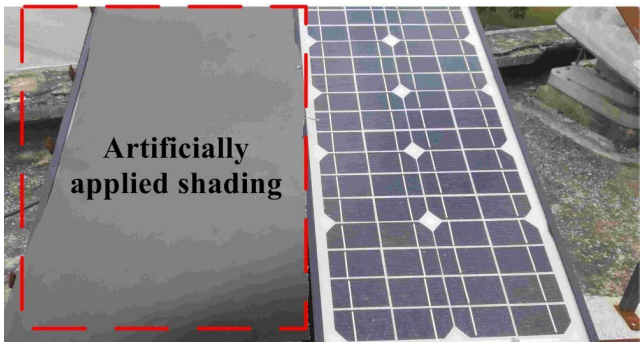

FIGURE 24. Practically applying artificial shading on PV module.

VII. CONCLUSION

In this work, a revised P&O approach with modified MPC controller to track the MPP is proposed. It is verified under different practical testing conditions and compared with the conventional P&O algorithm. After analyzing the results from both of the methods under different testing conditions we conclude that:

- Overshoot in PV power under a sudden increase in irradiation is minimized up to 35% of its original value in the worst case when compared with the conventional method.
- Undershoot in PV power under a sudden increase in irradiation is minimized up to 68% of its original value in the worst when compared with the conventional method.
- Settling time in PV power is reduced to 145 ms in worst case environmental conditions in contrast with the benchmarked method.
- The computational load is reduced because application of iRCS-MPC algorithm in the MPC controller block.

REFERENCES

[1] M. Abdel-Salam, M.-T. El-Mohandes, and M. Goda, "An improved perturb-and-observe based MPPT method for PV systems under varying irradiation levels," *Solar Energy*, vol. 171, pp. 547–561, Sep. 2018.
[2] M. A. G. de Brito, L. Galotto, L. P. Sampaio, G. E. de Azevedo e Melo, and C. A. Canesin, "Evaluation of the main MPPT techniques for photovoltaic applications," *IEEE Trans. Ind. Electron.*, vol. 60, no. 3, pp. 1156–1167, Mar. 2013.
[3] P. Sivakumar, A. A. Kader, Y. Kaliavaradhan, and M. Arutchelvi, "Analysis and enhancement of PV efficiency with incremental conductance MPPT technique under non-linear loading conditions," *Renew. Energy*, vol. 81, pp. 543–550, Sep. 2015.
[4] T. K. Soon and S. Mekhilef, "Modified incremental conductance MPPT algorithm to mitigate inaccurate responses under fast-changing solar irradiation level," *Sol. Energy*, vol. 101, pp. 333–342, Mar. 2014.
[5] R. Ahmad, A. F. Murtaza, and H. A. Sher, "Power tracking techniques for efficient operation of photovoltaic array in solar applications—A review," *Renew. Sustain. Energy Rev.*, vol. 101, pp. 82–102, Mar. 2019.
[6] A. Harrag and S. Messalti, "Variable step size modified P&O MPPT algorithm using GA-based hybrid offline/online PID controller," *Renew. Sustain. Energy Rev.*, vol. 49, pp. 1247–1260, Sep. 2015.
[7] M. A. Elgendy, B. Zahawi, and D. J. Atkinson, "Assessment of perturb and observe MPPT algorithm implementation techniques for PV pumping applications," *IEEE Trans. Sustain. Energy*, vol. 3, no. 1, pp. 21–33, Jan. 2012.
[8] E. Bianconi, J. Calvente, R. Giral, E. Mamarelis, G. Petrone, C. A. Ramos-Paja, G. Spagnuolo, and M. Vitelli, "A fast current-based MPPT technique employing sliding mode control," *IEEE Trans. Ind. Electron.*, vol. 60, no. 3, pp. 1168–1178, Mar. 2013.
[9] S. K. Kollimalla and M. K. Mishra, "A novel adaptive P&O MPPT algorithm considering sudden changes in the irradiance," *IEEE Trans. Energy Convers.*, vol. 29, no. 3, pp. 602–610, Sep. 2014.

[10] M. B. Shadmand, R. S. Balog, and H. Abu-Rub, "Model predictive control of PV sources in a smart DC distribution system: Maximum power point tracking and droop control," *IEEE Trans. Energy Convers.*, vol. 29, no. 4, pp. 913–921, Dec. 2014.
[11] H. A. Sher, A. F. Murtaza, A. Noman, K. E. Addoweesh, K. Al-Haddad, and M. Chiaberge, "A new sensorless hybrid MPPT algorithm based on fractional short-circuit current measurement and P&O MPPT," *IEEE Trans. Sustain. Energy*, vol. 6, no. 4, pp. 1426–1434, Oct. 2015.
[12] A. A. S. Mohamed, A. Berzoy, and O. A. Mohammed, "Design and hardware implementation of FL-MPPT control of PV systems based on GA and small-signal analysis," *IEEE Trans. Sustain. Energy*, vol. 8, no. 1, pp. 279–290, Jan. 2017.
[13] X. Li, H. Wen, Y. Hu, and L. Jiang, "A novel beta parameter based fuzzy-logic controller for photovoltaic MPPT application," *Renew. Energy*, vol. 130, pp. 416–427, Jan. 2019.
[14] P. P. Wang, D. Ruan, and E. E. Kerre, *Fuzzy Logic: A Spectrum of Theoretical and Practical Issues*, vol. 215. Berlin, Germany: Springer-Verlag, 2007.
[15] J. Ahmed and Z. Salam, "An improved perturb and observe (P&O) maximum power point tracking (MPPT) algorithm for higher efficiency," *Appl. Energy*, vol. 150, pp. 97–108, Jul. 2015.
[16] M. Al-Dhaifallah, A. M. Nassef, H. Rezk, and K. S. Nisar, "Optimal parameter design of fractional order control based INC-MPPT for PV system," *Sol. Energy*, vol. 159, pp. 650–664, Jan. 2018.
[17] N. E. Zakzouk, M. A. Elsaharty, A. K. Abdelsalam, A. A. Helal, and B. W. Williams, "Improved performance low-cost incremental conductance PV MPPT technique," *IET Renew. Power Gener.*, vol. 10, no. 4, pp. 561–574, Apr. 2016.
[18] H. A. Sher, A. Murtaza, A. Noman, K. E. Addoweesh, and M. Chiaberge, "An intelligent control strategy of fractional short circuit current maximum power point tracking technique for photovoltaic applications," *J. Renew. Sustain. Energy*, vol. 7, no. 1, 2015, Art. no. 013114.
[19] T.-W. Hsu, H.-H. Wu, D.-L. Tsai, and C.-L. Wei, "Photovoltaic energy harvester with fractional open-circuit voltage based maximum power point tracking circuit," *IEEE Trans. Circuits Syst., II, Exp. Briefs*, vol. 66, no. 2, pp. 257–261, Feb. 2019.
[20] D. Baimel, R. Shkoury, L. Elbaz, S. Tapuchi, and N. Baimel, "Novel optimized method for maximum power point tracking in PV systems using fractional open circuit voltage technique," in *Proc. Int. Symp. Power Electron., Elect. Drives, Autom. Motion (SPEEDAM)*, Jun. 2016, pp. 889–894.
[21] A. S. Samosir, H. Gusmedi, S. Purwiyanti, and E. Komalasari, "Modeling and simulation of fuzzy logic based maximum power point tracking (MPPT) for PV application," *Int. J. Electr. Comput. Eng.*, vol. 8, no. 3, pp. 1315–1323, 2018.
[22] A. Al Nabulsi and R. Dhaouadi, "Efficiency optimization of a DSP-based standalone PV system using fuzzy logic and dual-MPPT control," *IEEE Trans. Ind. Informat.*, vol. 8, no. 3, pp. 573–584, Aug. 2012.
[23] J. El Khazane and E. H. Tissir, "Achievement of MPPT by finite time convergence sliding mode control for photovoltaic pumping system," *Sol. Energy*, vol. 166, pp. 13–20, May 2018.
[24] P. E. Kakosimos and A. G. Kladas, "Implementation of photovoltaic array MPPT through fixed step predictive control technique," *Renew. Energy*, vol. 36, no. 9, pp. 2508–2514, 2011.
[25] P. Cortés, M. P. Kazmierkowski, R. M. Kennel, D. E. Quevedo, and J. Rodriguez, "Predictive control in power electronics and drives," *IEEE Trans. Ind. Electron.*, vol. 55, no. 12, pp. 4312–4324, Dec. 2008.
[26] J. Rodriguez, J. Pontt, C. A. Silva, P. Correa, P. Lezana, P. Cortés, and U. Ammann, "Predictive current control of a voltage source inverter," *IEEE Trans. Ind. Electron.*, vol. 54, no. 1, pp. 495–503, Feb. 2007.
[27] R. B. A. Cunha, R. Inomoto, J. A. T. Altuna, F. F. Costa, S. G. Di Santo, and A. J. S. Filho, "Constant switching frequency finite control set model predictive control applied to the boost converter of a photovoltaic system," *Solar Energy*, vol. 189, pp. 57–66, Sep. 2019.
[28] H. A. Sher, K. E. Addoweesh, and K. Al-Haddad, "An efficient and cost-effective hybrid MPPT method for a photovoltaic flyback microinverter," *IEEE Trans. Sustain. Energy*, vol. 9, no. 3, pp. 1137–1144, Jul. 2018.
[29] L. Piegari, R. Rizzo, I. Spina, and P. Tricoli, "Optimized adaptive perturb and observe maximum power point tracking control for photovoltaic generation," *Energies*, vol. 8, no. 5, pp. 3418–3436, 2015.

AFAQ HUSSAIN received the B.S. degree in electrical engineering from the National University of Computer and Emerging Sciences (FAST-NUCES), Islamabad, Pakistan, in 2017.

He is currently pursuing the M.Sc. degree in electronic engineering with the Ghulam Ishaq Khan Institute of Engineering Sciences and Technology (GIKI), Topi, Pakistan. His current research interests include efficient control of power electronic converter and renewable energy generation.

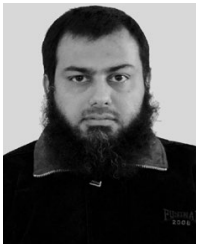

HADEED AHMED SHER (S'14–M'17–SM'19) received the B.Sc. degree in electrical engineering from Bahauddin Zakariya University, Multan, Pakistan, in 2005, the M.Sc. degree in electrical engineering from the University of Engineering and Technology, Lahore, Pakistan, in 2008, and the Ph.D. degree in electrical engineering from King Saud University (KSU), Riyadh, Saudi Arabia, in 2016.

He is currently an Assistant Professor with the Faculty of Electrical Engineering, Ghulam Ishaq Khan Institute of Engineering Sciences and Technology, Topi, Pakistan. His current research interests include grid connected solar photovoltaic systems, maximum power point tracking, and power electronics. He received the Research Excellence Award from the KSU College of Engineering for the year 2012 and 2015.

ALI FAISAL MURTAZA (M'16) received the B.Sc. degree from the National University of Sciences and Technology (NUST), Rawalpindi, Pakistan, the M.Sc. degree from the University of Engineering and Technology (UET), Lahore, Pakistan, and the Ph.D. degree from the Politecnico di Torino, Torino, Italy.

He is currently a Research Director and an Assistant Professor with the Faculty of Engineering, University of Central Punjab (UCP), Lahore, Pakistan. At UCP, a research group Efficient Electrical Energy Systems is active under his supervision. His current research interests include the design of solar photovoltaic (PV) systems, including DC micro-grids, DC-DC converters, I-V curve tracing, maximum power point trackers, and partial shading effects.

KAMAL AL-HADDAD (S'82–M'88–SM'92–F'07) received the B.Sc.A. and M.Sc.A. degrees in electrical engineering from the University of Québec à Trois-Riviéres, Canada, in 1982 and 1984, respectively, and the Ph.D. degree in electrical engineering from the Institute National Polytechnique, Toulouse, France, in 1988. Since 1990, he has been a Professor with the Electrical Engineering Department, École de Technologie SupÉrieure (ÉTS), Montreal, QC, Canada, where he has been the Canada Research Chair in electric energy conversion and power electronics, since 2002. He has supervised more than 170 Ph.D. and M.Sc.A. Students involved in the field of power electronics. He is a Consultant and has established very solid link with Canadian industries. He has coauthored more than 600 TRANSACTIONS and conference papers and two books. His current research interests include high-efficient static power converters, active-hybrid power filters, grid connect, and multilevel converters, including modeling, control, and development of prototypes for various industrial applications. Prof. Al-Haddad is a member of the Academy of Science, a Fellow of the Royal Society of Canada, and a Fellow Member of the Canadian Academy of Engineering. He was a recipient of the Dr.-Ing. Eugene Mittelmann Achievement Award. He was the IEEE IES President, from 2016 to 2017. He is an IES Distinguished Lecturer.